Editors' Suggestion | Featured in Physics

Realization of a Laughlin State of Two Rapidly Rotating Fermions

Philipp Lunt,[1,*] Paul Hill,[1] Johannes Reiter,[1] Philipp M. Preiss,[2,3] Maciej Gałka,[1] and Selim Jochim[1]
[1]Physikalisches Institut der Universität Heidelberg, Im Neuenheimer Feld 226, 69120 Heidelberg, Germany
[2]Max Planck Institute of Quantum Optics, Hans-Kopfermann-Str. 1, 85748 Garching, Germany
[3]Munich Center for Quantum Science and Technology (MCQST), Schellingstr. 4, 80799 München, Germany

(Received 20 February 2024; revised 31 May 2024; accepted 31 October 2024; published 16 December 2024)

We realize a Laughlin state of two rapidly rotating fermionic atoms in an optical tweezer. By utilizing a single atom and spin resolved imaging technique, we sample the Laughlin wave function thereby revealing its distinctive features, including a vortex distribution in the relative motion, correlations in the particles' relative angle, and suppression of the interparticle interactions. Our Letter lays the foundation for atom-by-atom assembly of fractional quantum Hall states in rotating atomic gases.

DOI: 10.1103/PhysRevLett.133.253401

Neutral particles in a rotating frame mimic the motion of charged particles subjected to a magnetic field [1]. The Coriolis force takes on the role of the Lorentz force, which dictates free particles to move on cyclotron orbits. Within a quantum mechanical framework, this results in quantized energy levels, referred to as Landau levels. They are infinitely degenerate in the case of translational invariance, separated by the large cyclotron frequency. The properties of such a system are classified by the filling factor ν, which is defined as the ratio of the particle number and the number of states per Landau level [2]. For integer values, the Landau levels are completely occupied, resulting in the integer quantum Hall effect [3], while for $\nu < 1$ the lowest Landau level (LLL) is partially filled leading to the emergence of strongly correlated phases including fractional quantum Hall states [4,5]. The fractional filling factors $\nu = 1/m$, with an integer m, are qualitatively described by Laughlin's wave function [6].

Rotating ultracold atomic gases [7,8] is one approach among other techniques [9–18] to study quantum many-body physics in magnetic fields. In the slow-rotation limit of large filling factors $\nu \gg 1$ quantized flux vortices are formed [19] and arrange in a triangular Abrikosov lattice [20,21]. Reaching filling factors $\nu \sim 100$ has been achieved with ultracold Bose gases, signaled by the softening of the Abrikosov lattice [22,23] and more recently by distilling a single Landau gauge wave function in the LLL [24–26]. In the limit of rapid rotation $\nu \lesssim 1$ strongly correlated phases are predicted analogous to phases occurring in the fractional quantum Hall effect [7,27–29], where first attempts have been pursued in rotating atomic clusters of interacting bosons [30]; in different systems, Laughlin states with two photons [31] and with two bosonic atoms in a driven optical lattice [32] have been realized lately. Ultracold Fermi gases at filling factors $\nu \lesssim 1$ have thus far been unexplored experimentally due to challenges to transfer fermions to the LLL via rotation of the potential, given the Pauli exclusion principle.

In this Letter, we realize the $\nu = 1/2$ Laughlin state of two rapidly rotating spinful fermions in an optical tweezer. Our approach relies on the smooth rotation of the optical

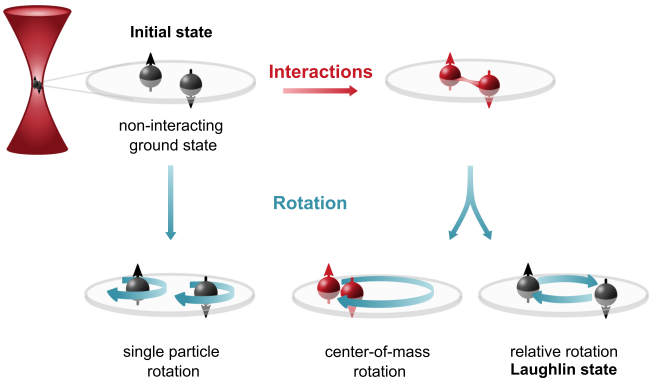

FIG. 1. Conceptual path to a Laughlin state with two rapidly rotating fermions. Two spinful noninteracting fermions (black particles) are prepared in the ground state of a radially symmetric optical tweezer. To couple the particles to states with angular momentum, we tune the trap to an elliptical shape that rotates. Rotating the non-interacting particles leads to independent, single-particle rotation. Interactions (indicated by red) break the symmetry between the particles' center-of-mass and relative motion since the interactions only couple to the relative part of the wave function. Hence, states with angular momentum only in the center-of-mass degree of freedom have different energy than states with the same angular momentum in the relative motion and thus both can be selectively addressed with different rotation frequencies. States with angular momentum only in the relative degree of freedom are Laughlin states. These states possess a node in their relative wave function which, in our case of contact interactions, renders them noninteracting.

*Contact author: lunt@physi.uni-heidelberg.de

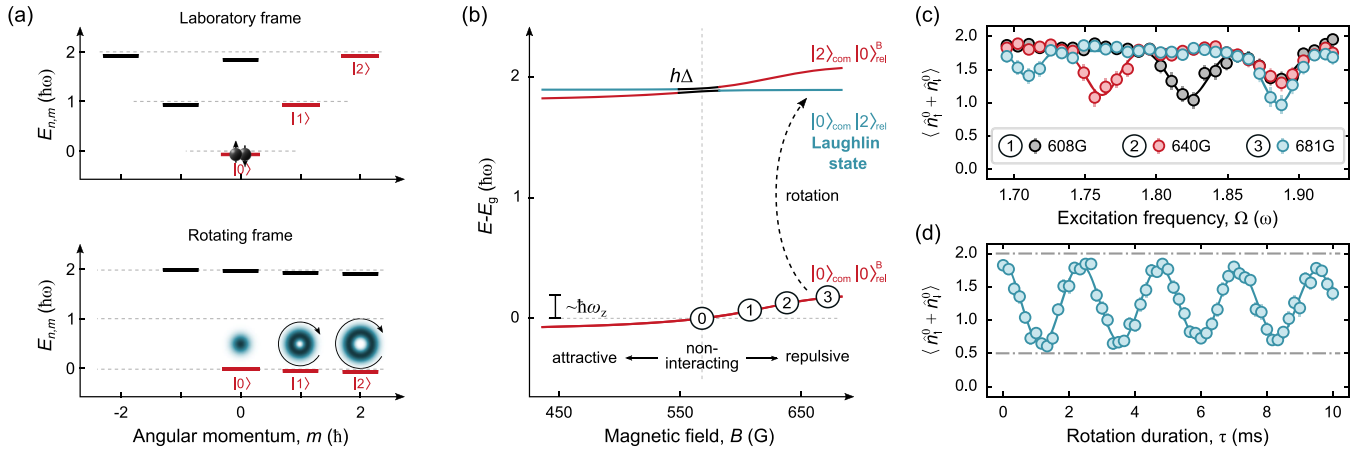

FIG. 2. Preparation of the Laughlin state. (a) Two noninteracting fermions are prepared in the ground state of the optical tweezer (top). In-plane it forms an approximate harmonic oscillator. States $|m\rangle$ (red) with maximal angular momentum along the axial direction $L_z = m\hbar$ in their respective shell n ($n = m$) form the lowest Landau level in the rotating frame with ω, i.e., the deconfinement limit (bottom). (b) Energy spectrum in the laboratory frame in the $L_z = 0\hbar, 2\hbar$ angular momentum manifold of two interacting fermions in a cigar-shaped harmonic trap including an anharmonicity Δ. Adiabatic tuning of the magnetic field ⓪ → ③ leads to an energy shift E_{int} with respect to the noninteracting ground state energy E_g (horizontal dotted line); the maximum E_{int} is on the order of the axial trap frequency ω_z. In the $L_z = 2\hbar$ manifold in the limit $E_{\mathrm{int}} \gg \Delta$, the two states correspond to $|2\rangle_{\mathrm{com}}|0\rangle_{\mathrm{rel}}$ and $|0\rangle_{\mathrm{com}}|2\rangle_{\mathrm{rel}}$ in the center-of-mass and relative basis, with the latter being the Laughlin state $|\psi_{1/2}\rangle$. (c) Excitation spectrum at various magnetic fields measured by counting the remaining atoms in the single-particle ground state $\langle \hat{n}^0_\uparrow + \hat{n}^0_\downarrow \rangle$ after applying the rotating perturbation for $\tau = 350$ μs. For increasingly repulsive interacting atoms, the frequency of the relative excitation $\Omega_{\mathrm{rel}} < 1.9\omega$ decreases, while the frequency of center-of-mass excitation at $\Omega_{\mathrm{com}} \sim 1.9\omega$ stays approximately constant. (d) Rabi oscillations at 680G on the resonance $\Omega_{\mathrm{rel}} \approx 1.7\omega$ driven with a Rabi rate $\Omega_{\mathrm{rabi}}/2\pi \approx 0.42$ kHz. According to Eq. (2b) the Rabi oscillations reach 2 and 0.5 (dashed lines). The error bars in (c),(d) represent the standard error of the mean and are smaller than the data points if not visible.

potential and precise control of the in-plane anisotropy to a level of 4×10^{-4} [33]. On a conceptual level, the realization of the Laughlin state requires interactions between the particles and a strong magnetic field here engineered via rotation, illustrated in Fig. 1. In the absence of interactions, rotation of the particles leads to independent, single-particle rotation. In this scenario, the center-of-mass and relative motion of the particles are identical. The interactions break the symmetry between the particles' center-of-mass and relative motion (defining the preferred basis) since they couple only to the relative part of the wave function. The interaction energy of a state with only center-of-mass angular momentum tunes differently compared to a state with relative angular momentum, allowing for selective spectroscopic addressing.

The Laughlin state for any particle number N incorporates angular momentum in the relative motion between each and every particle, thereby suppressing the interaction energy. The spatial part of the Laughlin wave function is described by

$$\psi_{1/m}(z_1, \ldots, z_N) = \prod_{i<j} (z_i - z_j)^m e^{-\sum_{i=1}^{N} |z_i|^2/2}, \quad (1)$$

where $z_j = (x_j + iy_j)/l_{\mathrm{HO}}$ labels the complex coordinate of the jth particle in the radial plane in units of the harmonic oscillator length l_{HO}, which defines the natural length scale of our system, m is the angular momentum in units of $\hbar$ incorporated in the relative motion of the particles $(z_i - z_j)$, and the filling factor relates via $\nu = 1/m$. In our two-particle case of a spin singlet, the spatial wave function is required to be symmetric, thereby restricting the exponent m to even numbers. In the many-body limit, our system connects to spinful fractional quantum Hall states described by the Halperin wave function, which is a generalization of the Laughlin wave function containing a spin degree of freedom [39].

Preparation of the Laughlin state—We start by preparing a noninteracting spin-up and -down fermion of ^{6}Li atoms in the ground state of a radially symmetric, tightly focused optical tweezer [40]. The tweezer forms a cigar-shaped harmonic trap with the radial $\omega/2\pi \approx 7.9$ kHz and axial $\omega_z/2\pi \approx 7.9$ kHz trap frequency, determining $l_{\mathrm{HO}} = \sqrt{\hbar/m_{\mathrm{Li}}\omega}$. Since the rotation couples only to the in-plane motion, we consider a two-dimensional (2D) potential in Fig. 2(a), top, which forms a rotationally symmetric 2D harmonic oscillator up to small anharmonic corrections. The energies $E_{n,m}$ are labeled by their shell number n and their angular momentum $L_z = m\hbar$ along the axial direction. When viewed in the reference frame rotating at ω, the states remain eigenstates of the system, yet the energy rearranges such that the eigenstates form degenerate Landau levels, shown in Fig. 2(a), bottom. The states $|m\rangle$ (red states) with maximal angular momentum in each shell, i.e., $n = m$, belong to the LLL [33].

To excite the atoms selectively to angular momentum eigenstates in the LLL, we interfere the tweezer with a Laguerre-Gaussian beam which deforms the originally radially symmetric potential and acts as a rotating perturbation $\propto (z^l e^{-i\Omega t} + \text{H.c.})$. It couples states that differ in angular momentum by $\hbar l$ and in energy by $\hbar\Omega$. Here, $2\pi l$ is the phase winding of the Laguerre-Gaussian beam, and Ω/l is the angular rotation frequency of the optical potential set by the angular frequency difference Ω between the tweezer and the perturbation beam. To realize the $\nu = 1/2$ Laughlin state, we introduce a total angular momentum of $2\hbar$ using the Laguerre-Gaussian beam with $l = 2$ [41].

Our approach to reach the two-particle Laughlin state $|\psi_{1/2}\rangle$ is illustrated in Fig. 2(b). We outline the relevant energy levels of two contact-interacting fermions trapped in a cigar-shaped potential, viewed in the laboratory frame. We express the eigenstates in the center-of-mass and relative coordinates, as the interactions depend only on the relative motion and the center-of-mass and relative degrees of freedom decouple in a harmonic potential. The decoupling also holds in the presence of the weak anharmonicity $\Delta \approx 1.4$ kHz in the limit of large interaction energy $E_{\text{int}}/h \gg \Delta$.

The normalized spatial wave function of the two-particle Laughlin state $|\psi_{1/2}\rangle$ can be expressed using harmonic oscillator eigenstates

$$|\psi_{1/2}\rangle = |0\rangle_{\text{com}}|2\rangle_{\text{rel}} \tag{2a}$$

$$= (|0\rangle_\uparrow|2\rangle_\downarrow + |2\rangle_\uparrow|0\rangle_\downarrow)/2 - |1\rangle_\uparrow|1\rangle_\downarrow/\sqrt{2}, \tag{2b}$$

in the center-of-mass and relative basis [Eq. (2a)] and the single-particle basis [Eq. (2b)]. The Laughlin state $|\psi_{1/2}\rangle$ remains in the center-of-mass ground state, while carrying $2\hbar$ angular momentum in the relative degree of freedom. In the single-particle basis, $|\psi_{1/2}\rangle$ is a superposition of states in the LLL, where either one spin state carries $2\hbar$ angular momentum leaving the other spin state in the ground state or each spin state carries $1\hbar$ angular momentum. Note, that we directly relate each particle to a spin value via the subscripts $\uparrow, \downarrow$ [42].

We spectroscopically characterize the system by measuring the single-particle occupation number in the ground state $\langle \hat{n}^0_\uparrow + \hat{n}^0_\downarrow \rangle$ after applying the rotating perturbation for $\tau = 350$ μs at different interactions strengths, shown in Fig. 2(c). For those repulsive interactions, we observe two resonances which correspond to the center-of-mass $|2\rangle_{\text{com}}|0\rangle^{\text{B}}_{\text{rel}}$ and relative rotation $|0\rangle_{\text{com}}|2\rangle_{\text{rel}}$ (for $E_{\text{int}}/h \gg \Delta$). Here, $|0\rangle^{\text{B}}_{\text{rel}}$ labels the ground state in the relative motion which changes with the interaction strength tuned by the magnetic field. As the interaction energy depends only on the relative motion, the resonance frequency of the center-of-mass excitation tunes similarly to the ground state energy and thus stays approximately constant at $\Omega_{\text{com}} \sim 1.9\omega$, down-shifted from 2ω due to the anharmonicities. In contrast, the relative excitation $\Omega_{\text{rel}} < 1.9\omega$ shifts to lower frequencies for larger repulsive interaction strengths. Modeling the energy levels in the trap allows us to subtract the interaction-dependent ground state energy, showing the suppression of interparticle interactions in the $|0\rangle_{\text{com}}|2\rangle_{\text{rel}}$ state (see also Fig. S2 in [33]).

By ramping the magnetic field to 680G, we reach the limit $E_{\text{int}}/h \approx 9.9$ kHz $\gg \Delta$. In Fig. 2(d), we show Rabi oscillations with a Rabi rate $\Omega_{\text{rabi}}/2\pi \approx 0.42$ kHz on the resonance $\Omega \approx 1.7\omega$ between the repulsively interacting ground state and the Laughlin state, to which we transfer via a π pulse. Since we measure $\langle \hat{n}^0_\uparrow + \hat{n}^0_\downarrow \rangle$ we expect the minimum of the Rabi oscillations to reach 0.5, following Eq. (2b). An upper bound of the preparation fidelity is inferred through the single-particle ground state occupation after half a Rabi cycle $\mathcal{F}_{\text{prep}} = 96(2)\%$, also accounting for the preparation fidelity of two atoms in the ground state.

Furthermore, we measure the lifetime of the Laughlin state by utilizing Ramsey spectroscopy which yields $\tau_{\text{coh}} = 191(21)$ ms [33]. Remarkably, this corresponds to 21 400 coherent rotations of the particles, demonstrating that the Laughlin state is insensitive to environmental noise sources.

Observation of the Laughlin wave function—We measure the density of the Laughlin wave function in momentum space after a time-of-flight expansion of $t_{\text{tof}} = 1.78$ ms from approximately 11 000 experimental realizations using a spin and atom resolved fluorescence imaging technique [43]. Since the Laughlin state consists of states in the LLL and suppresses interactions the expansion corresponds to a magnification of the initial wave function [44]. We express all momenta in units of the harmonic oscillator momentum $p_{\text{HO}} = \sqrt{\hbar m\omega}$.

In Fig. 3(a), we show the normalized density in the single particle basis of the spin up and spin down fermion. In that basis, neither of the spin states exhibits a vortex distribution. Instead, the density has a flattened profile. Note that the density distribution of the spin-up state is larger stemming from off-resonant scattering during the prior imaging of the spin-down state [33].

In order to reveal the key signatures of the Laughlin wave function we transform to the center-of-mass and relative basis. In each experimental realization, we measure the momentum $\mathbf{p} = (p_x, p_y)$ of the spin-up and spin-down fermion, denoted as $\mathbf{p}_\uparrow$ and $\mathbf{p}_\downarrow$, respectively. This allows us to calculate the center-of-mass $\mathbf{p}_{\text{com}} = 1/\sqrt{2}(\mathbf{p}_\uparrow + \mathbf{p}_\downarrow)$ and relative $\mathbf{p}_{\text{rel}} = 1/\sqrt{2}(\mathbf{p}_\uparrow - \mathbf{p}_\downarrow)$ coordinates in a single snapshot of the wave function. We determine the normalized density in the center-of-mass and relative basis in Fig. 3(b), revealing the striking features of the Laughlin wave function.

While in center-of-mass coordinates the density distribution of the Laughlin state has a Gaussian shape, it shows a rotationally symmetric vortex distribution in relative

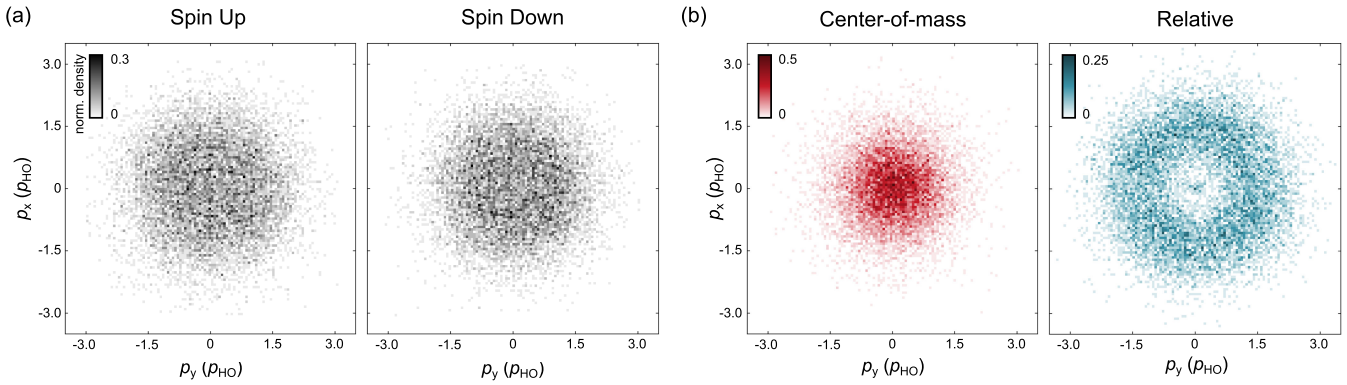

FIG. 3. Laughlin wave function of two rapidly rotating fermions. (a) Normalized single-particle density of the spin-up and spin-down atom. Both densities flatten out for small momenta. (b) Normalized density in center-of-mass coordinates $\mathbf{p}_{\mathrm{com}} = 1/\sqrt{2}(\mathbf{p}_\uparrow + \mathbf{p}_\downarrow)$ and in relative coordinates $\mathbf{p}_{\mathrm{rel}} = 1/\sqrt{2}(\mathbf{p}_\uparrow - \mathbf{p}_\downarrow)$. The center-of-mass motion has a Gaussian shape. The angular momentum is incorporated in the relative motion of the particles, resulting in an azimuthally symmetric vortex distribution of the density. The total angular momentum of $2\hbar$ determines the maximum of the vortex distribution at a radius of $\sqrt{2}p_{\mathrm{HO}}$. Note that a small admixture $\sim$1% of a Feshbach molecule is visible as a peak at zero relative momenta.

coordinates owing to the angular momentum incorporated in the relative motion of the particles. The amount of angular momentum $m = 2\hbar$ determines the size of the vortex, with the peak density occurring at $\sqrt{2}p_{\mathrm{HO}}$. A small peak in the density at zero momenta is visible, stemming from anharmonic coupling to molecular states with center-of-mass excitations during the ramp of the magnetic field [45].

In Fig. 4, we compare our experimental data to theoretical predictions based on the Laughlin wave function $\psi_{1/2}$. In Figs. 4(a) and 4(b), we show the azimuthally averaged density distributions n_{p} as a function of the radial momentum $p_{\mathrm{r}} = \sqrt{p_{\mathrm{x}}^2 + p_{\mathrm{y}}^2}$, in both the single-particle basis and center-of-mass and relative basis, respectively. In the single-particle basis, the Laughlin state is a superposition of states in the LLL, according to Eq. (2b). In the center-of-mass and relative basis, the Laughlin state remains in the ground state $|0\rangle_{\mathrm{com}}$ (red) and occupies the $|2\rangle_{\mathrm{rel}}$ state (blue), respectively, according to Eq. (2a). The measured densities qualitatively agree with the theoretical predictions (solid lines) without free parameters. Additionally, we gain information about the phase of the wave function by letting the system evolve in a slightly anisotropic potential; the time evolution is consistent with the expected phase winding of 4π corresponding to an angular momentum of $2\hbar$ (see Fig. S3 in [33]).

Furthermore, we extract the relative angle correlations between the fermions, similar to [31]. For that, we subtract the azimuthal angle of the spin-up and -down atom

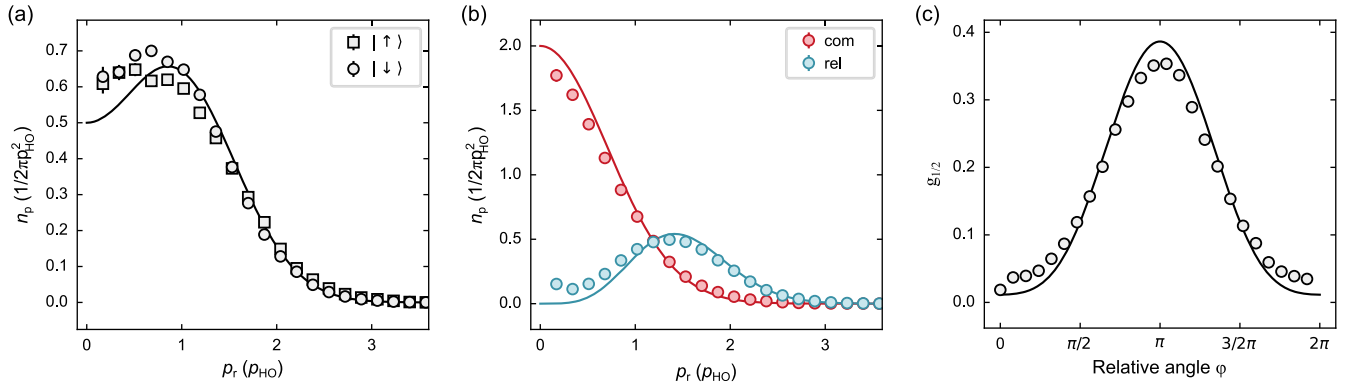

FIG. 4. Properties of the Laughlin state. (a) Radial densities of the spin-up and spin-down fermion. The solid line is a mixture of the states $|0\rangle, |1\rangle, |2\rangle$, according to Eq. (2b). (b) The Laughlin state remains in the ground state $|0\rangle_{\mathrm{com}}$ in center-of-mass coordinates, and occupies the $|2\rangle_{\mathrm{rel}}$ state in relative coordinates. The relative density is not zero at small momenta due to the admixture of a Feshbach molecule. The solid lines are calculated according to Eq. (2a). (c) Normalized histogram of relative angle correlations between the spin-up and spin-down fermion. The solid line is the theoretical angle correlation function $g_{1/2}(\varphi)$, see text. Error bars of the 95% confidence interval, determined using a bootstrapping technique, are smaller than the point size if not visible.

determined in each experimental realization and calculate the normalized angle distribution, shown in Fig. 4(c). The solid line represents the theoretical angle correlations of the $\nu = 1/2$ Laughlin wave function $g_{1/2}(\varphi) = (6 - 3\pi\cos\varphi + 4\cos^2\varphi)/16\pi$, without free parameters. In general, the Laughlin wave function $\psi_{1/m}$ exhibits a distinctive peak at a relative angle $\varphi = \pi$ between two particles, which becomes sharper with increasing angular momentum m [33]. In the context of our zero-range contact interactions, this observation demonstrates that while the Laughlin state is noninteracting due to the node in the particles' relative wave function, it is strongly correlated in the motional degree of freedom.

To connect to the electronic fractional quantum Hall effect, we emphasize that the Laughlin state, which is an excited eigenstate of the system in the laboratory frame, becomes the ground state in the reference frame rotating at the deconfinement limit. In order to further relate the two-particle Laughlin wave function to the many-body limit, we consider the density $\tilde{n}_\mathrm{p} = n_{\mathrm{p}\uparrow} + n_{\mathrm{p}\downarrow}$ at its center. Since the two-particle Laughlin wave function is an eigenstate of the harmonic oscillator, the momentum space $\tilde{n}_\mathrm{p}$ and real space $\tilde{n}_\mathrm{r}$ densities are the same $2\pi\tilde{n}_\mathrm{p}(p_r \to 0)p_\mathrm{B}^2 = 2\pi\tilde{n}_r(r \to 0)l_\mathrm{B}^2$ when expressed in units of the magnetic momentum p_B and magnetic length l_B, which in our analogous system are $p_\mathrm{B} = \sqrt{2}p_\mathrm{HO}$ and $l_\mathrm{B} = l_\mathrm{HO}/\sqrt{2}$. The measured value $2\pi\tilde{n}_\mathrm{p}(p_r \to 0)p_\mathrm{B}^2 \approx 0.6$ is close to the expected value of $1/2$, marking the precursor of the incompressible bulk plateau of the fractional quantum Hall droplet, extending up to a radius $2\sqrt{(N-1)}l_\mathrm{B}$ [7]. In this region, the density increases before it falls off to zero on a scale of l_B, indicating the onset of the compressibility of the edge in the many-body limit [5].

Conclusion and outlook—We directly observe microscopic correlations of the $\nu = 1/2$ Laughlin wave function demonstrating its noninteracting, yet strongly correlated nature due to the incorporation of angular momentum in the relative motion of the contact-interacting fermions. Our platform opens up a new pathway to explore microscopic details of spinful fractional quantum Hall states with ultracold atoms. Future work involves the scalability to larger particle numbers to study the emergence of topological phases of matter [46,47], the exploration of quantum Hall ferromagnetism [48,49], or the investigation of topologically distinct quantum phase transitions in the BEC-BCS crossover [50–52].

Acknowledgments—We gratefully acknowledge insightful discussions with Lauriane Chomaz, Fabian Grusdt, and Nathan Goldman. This work has been supported by the Heidelberg Center for Quantum Dynamics, the DFG Collaborative Research Centre SFB 1225 (ISOQUANT), Germany's Excellence Strategy EXC2181/1-390900948 (Heidelberg Excellence Cluster STRUCTURES) and the European Union's Horizon 2020 research and innovation program under Grant Agreements No. 817482 (PASQuanS), No. 725636 (ERC QuStA), and No. 948240 (ERC UniRand). This work has been partially financed by the Baden-Württemberg Stiftung.

P. L. led the experimental work, with significant contributions from P. H. P. L., P. H., J. R., and M. G. conducted the experiment. P. H. performed guiding theoretical studies. P. M. P. conceived the original ideas. P. M. P., M. G., and S. J. supervised the project. P. L., M. G., and P. H. wrote the manuscript with input from all authors. All authors contributed to the discussion of the results.

[1] J. Dalibard, Introduction to the physics of artificial gauge fields, in *Quantum Matter at Ultralow Temperatures*, Proceedings of the International School of Physics Enrico Fermi, edited by M. Inguscio, W. Ketterle, S. Stringari, and G. Roati (IOS Press, Amsterdam, Oxford, Tokio, Washington DC, 2016), pp. 1–61.

[2] G. Giuliani and G. Vignale, *Quantum Theory of the Electron Liquid* (Cambridge University Press, Cambridge, England, 2012).

[3] K. v. Klitzing, G. Dorda, and M. Pepper, New method for high-accuracy determination of the fine-structure constant based on quantized Hall resistance, Phys. Rev. Lett. **45**, 494 (1980).

[4] D. C. Tsui, H. L. Stormer, and A. C. Gossard, Two-dimensional magnetotransport in the extreme quantum limit, Phys. Rev. Lett. **48**, 1559 (1982).

[5] X.-G. Wen, *Quantum Field Theory of Many-Body Systems: From the Origin of Sound to an Origin of Light and Electrons* (Oxford University Press, Oxford, 2004).

[6] R. B. Laughlin, Anomalous quantum Hall effect: An incompressible quantum fluid with fractionally charged excitations, Phys. Rev. Lett. **50**, 1395 (1983).

[7] N. R. Cooper, Rapidly rotating atomic gases, Adv. Phys. **57**, 539 (2008).

[8] A. L. Fetter, Rotating trapped Bose-Einstein condensates, Rev. Mod. Phys. **81**, 647 (2009).

[9] Y.-J. Lin, K. Jiménez-García, and I. B. Spielman, Spin–orbit-coupled Bose–Einstein condensates, Nature (London) **471**, 83 (2011).

[10] T. Chalopin, T. Satoor, A. Evrard, V. Makhalov, J. Dalibard, R. Lopes, and S. Nascimbene, Probing chiral edge dynamics and bulk topology of a synthetic Hall system, Nat. Phys. **16**, 1017 (2020).

[11] M. Mancini, G. Pagano, G. Cappellini, L. Livi, M. Rider, J. Catani, C. Sias, P. Zoller, M. Inguscio, M. Dalmonte, and L. Fallani, Observation of chiral edge states with neutral fermions in synthetic Hall ribbons, Science **349**, 1510 (2015).

[12] T.-W. Zhou, G. Cappellini, D. Tusi, L. Franchi, J. Parravicini, C. Repellin, S. Greschner, M. Inguscio, T. Giamarchi, M. Filippone, J. Catani, and L. Fallani, Observation of universal Hall response in strongly interacting Fermions, Science **381**, 427 (2023).

[13] J. Struck, C. Ölschläger, M. Weinberg, P. Hauke, J. Simonet, A. Eckardt, M. Lewenstein, K. Sengstock, and P. Windpassinger, Tunable gauge potential for neutral and spinless particles in driven optical lattices, Phys. Rev. Lett. **108**, 225304 (2012).

[14] M. Aidelsburger, M. Lohse, C. Schweizer, M. Atala, J. T. Barreiro, S. Nascimbène, N. R. Cooper, I. Bloch, and N. Goldman, Measuring the Chern number of Hofstadter bands with ultracold bosonic atoms, Nat. Phys. **11**, 162 (2014).

[15] G. Jotzu, M. Messer, R. Desbuquois, M. Lebrat, T. Uehlinger, D. Greif, and T. Esslinger, Experimental realization of the topological Haldane model with ultracold fermions, Nature (London) **515**, 237 (2014).

[16] C. J. Kennedy, W. C. Burton, W. C. Chung, and W. Ketterle, Observation of Bose-Einstein condensation in a strong synthetic magnetic field, Nat. Phys. **11**, 859 (2015).

[17] M. E. Tai, A. Lukin, M. Rispoli, R. Schittko, T. Menke, D. Borgnia, P. M. Preiss, F. Grusdt, A. M. Kaufman, and M. Greiner, Microscopy of the interacting Harper-Hofstadter model in the two-body limit, Nature (London) **546**, 519 (2017).

[18] L. Asteria, D. T. Tran, T. Ozawa, M. Tarnowski, B. S. Rem, N. Fläschner, K. Sengstock, N. Goldman, and C. Weitenberg, Measuring quantized circular dichroism in ultracold topological matter, Nat. Phys. **15**, 449 (2019).

[19] K. W. Madison, F. Chevy, W. Wohlleben, and J. Dalibard, Vortex formation in a stirred Bose-Einstein condensate, Phys. Rev. Lett. **84**, 806 (2000).

[20] J. R. Abo-Shaeer, C. Raman, J. M. Vogels, and W. Ketterle, Observation of vortex lattices in Bose-Einstein condensates, Science **292**, 476 (2001).

[21] M. W. Zwierlein, J. R. Abo-Shaeer, A. Schirotzek, C. H. Schunck, and W. Ketterle, Vortices and superfluidity in a strongly interacting Fermi gas, Nature (London) **435**, 1047 (2005).

[22] V. Schweikhard, I. Coddington, P. Engels, V. P. Mogendorff, and E. A. Cornell, Rapidly rotating Bose-Einstein condensates in and near the lowest Landau level, Phys. Rev. Lett. **92**, 040404 (2004).

[23] V. Bretin, S. Stock, Y. Seurin, and J. Dalibard, Fast rotation of a Bose-Einstein condensate, Phys. Rev. Lett. **92**, 050403 (2004).

[24] R. J. Fletcher, A. Shaffer, C. C. Wilson, P. B. Patel, Z. Yan, V. Crépel, B. Mukherjee, and M. Zwierlein, Geometric squeezing into the lowest Landau level, Science **372**, 1318 (2021).

[25] B. Mukherjee, A. Shaffer, P. B. Patel, Z. Yan, C. C. Wilson, V. Crépel, R. J. Fletcher, and M. Zwierlein, Crystallization of bosonic quantum Hall states in a rotating quantum gas, Nature (London) **601**, 58 (2022).

[26] R. Yao, S. Chi, B. Mukherjee, A. Shaffer, M. Zwierlein, and R. J. Fletcher, Observation of chiral edge transport in a rapidly-rotating quantum gas, arXiv:2304.10468.

[27] N. R. Cooper, N. K. Wilkin, and J. M. F. Gunn, Quantum phases of vortices in rotating Bose-Einstein condensates, Phys. Rev. Lett. **87**, 120405 (2001).

[28] M. Popp, B. Paredes, and J. I. Cirac, Adiabatic path to fractional quantum Hall states of a few bosonic atoms, Phys. Rev. A **70**, 053612 (2004).

[29] N. Regnault and Th. Jolicoeur, Quantum Hall fractions in rotating Bose-Einstein condensates, Phys. Rev. Lett. **91**, 030402 (2003).

[30] N. Gemelke, E. Sarajlic, and S. Chu, Rotating few-body atomic systems in the fractional quantum Hall regime, arXiv:1007.2677.

[31] L. W. Clark, N. Schine, C. Baum, N. Jia, and J. Simon, Observation of Laughlin states made of light, Nature (London) **582**, 41 (2020).

[32] J. Léonard, S. Kim, J. Kwan, P. Segura, F. Grusdt, C. Repellin, N. Goldman, and M. Greiner, Realization of a fractional quantum Hall state with ultracold atoms, Nature (London) **619**, 495 (2023).

[33] See Supplemental Material at http://link.aps.org/supplemental/10.1103/PhysRevLett.133.253401 for experimental details, data processing, and theoretical analysis, which includes Refs. [34–38].

[34] N. K. Wilkin, J. M. F. Gunn, and R. A. Smith, Do attractive bosons condense?, Phys. Rev. Lett. **80**, 2265 (1998).

[35] Zbigniew Idziaszek and Tommaso Calarco, Analytical solutions for the dynamics of two trapped interacting ultracold atoms, Phys. Rev. A **74**, 022712 (2006).

[36] M. Mamaev, J. H. Thywissen, and A. M. Rey, Quantum computation toolbox for decoherence-free qubits using multiband alkali atoms, Adv. Quantum Technol. **3**, 1900132 (2020).

[37] Thomas Hartke, Botond Oreg, Ningyuan Jia, and Martin Zwierlein, Quantum register of fermion pairs, Nature (London) **601**, 537 (2022).

[38] M. Holten, L. Bayha, K. Subramanian, S. Brandstetter, C. Heintze, P. Lunt, P. M. Preiss, and S. Jochim, Observation of Cooper pairs in a mesoscopic two-dimensional Fermi gas, Nature (London) **606**, 287 (2022).

[39] B. I. Halperin, Theory of the quantized Hall conductance, Helv. Phys. Acta **56**, 75 (1983), https://ncatlab.org/nlab/files/Halperin-TheoryOfQHE.pdf.

[40] F. Serwane, G. Zürn, T. Lompe, T. B. Ottenstein, A. N. Wenz, and S. Jochim, Deterministic preparation of a tunable few-Fermion system, Science **332**, 336 (2011).

[41] Philipp Lunt, Paul Hill, Johannes Reiter, Philipp M. Preiss, Maciej Gałka, and Selim Jochim, companion paper, Engineering single-atom angular momentum eigenstates in an optical tweezer, Phys. Rev. A **110**, 063315 (2024).

[42] We prepare a spin singlet state $|\Psi\rangle = 1/\sqrt{2}(|\uparrow\downarrow\rangle - |\downarrow\uparrow\rangle) \otimes |\psi_{1/2}\rangle$ in each experimental realization. Since we do not couple to the spin degree of freedom and our fluorescence imaging measures in the $\{|\downarrow\rangle, |\uparrow\rangle\}$ basis, the wave function in Eq. (2b) describes the spatial wave function after relating each particle to its spin value.

[43] A. Bergschneider, V. M. Klinkhamer, J. H. Becher, R. Klemt, G. Zürn, P. M. Preiss, and S. Jochim, Spin-resolved single-atom imaging of ^{6}Li in free space, Phys. Rev. A **97**, 063613 (2018).

[44] N. Read and N. R. Cooper, Free expansion of lowest-Landau-level states of trapped atoms: A wave-function microscope, Phys. Rev. A **68**, 035601 (2003).

[45] S. Sala, G. Zürn, T. Lompe, A. N. Wenz, S. Murmann, F. Serwane, S. Jochim, and A. Saenz, Coherent molecule formation in anharmonic potentials near confinement-induced resonances, Phys. Rev. Lett. **110**, 203202 (2013).

[46] F. A. Palm, J. Kwan, B. Bakkali-Hassani, M. Greiner, U. Schollwöck, N. Goldman, and F. Grusdt, Growing extended laughlin states in a quantum gas microscope: A patchwork construction, Phys. Rev. Res. **6**, 013198 (2024).
[47] F. Letscher, F. Grusdt, and M. Fleischhauer, Growing quantum states with topological order, Phys. Rev. B **91**, 184302 (2015).
[48] L. Palm, F. Grusdt, and P. M. Preiss, Skyrmion ground states of rapidly rotating few-fermion systems, New J. Phys. **22**, 083037 (2020).
[49] K. Yang, K. Moon, L. Zheng, A. H. MacDonald, S. M. Girvin, D. Yoshioka, and S. C. Zhang, Quantum ferromagnetism and phase transitions in double-layer quantum Hall systems, Phys. Rev. Lett. **72**, 732 (1994).
[50] K. Yang and H. Zhai, Quantum Hall transition near a fermion Feshbach resonance in a rotating trap, Phys. Rev. Lett. **100**, 030404 (2008).
[51] C. Repellin, T. Yefsah, and A. Sterdyniak, Creating a bosonic fractional quantum Hall state by pairing fermions, Phys. Rev. B **96**, 161111(R) (2017).
[52] T. Ho, Fusing quantum Hall states in cold atoms, arXiv: 1608.00074.